Journal of Power Sources 197 (2012) 107–110

Contents lists available at SciVerse ScienceDirect

Journal of Power Sources

journal homepage: www.elsevier.com/locate/jpowsour

Short communication

Size effect of silver nanoclusters on their catalytic activity for oxygen electro-reduction

Yizhong Lu [a,b], Wei Chen [a,*]

[a] State Key Laboratory of Electroanalytical Chemistry, Changchun Institute of Applied Chemistry, Chinese Academy of Sciences, Changchun 130022, Jilin, China
[b] Graduate School of the Chinese Academy of Sciences, Beijing 100039, China

ARTICLE INFO

Article history:
Received 27 July 2011
Received in revised form
12 September 2011
Accepted 13 September 2011
Available online 19 September 2011

Keywords:
Electrocatalysis
Nanoclusters
Oxygen reduction
Rotating disk electrode
Silver
Voltammetry

ABSTRACT

Two different sized silver nanoclusters are prepared by two different synthetic routs. First, a small nanocluster (NC) which is 0.7 nm in diameter was synthesized by using meso-2, 3-dimercapto-succinic acid (DMSA) as a capping ligand, and second a larger nanoparticle (NP) which is 3.3 nm in diameter was prepared by chemical reduction and coated with DMSA. The as-prepared silver nanoclusters or nanoparticles are then loaded onto a glassy carbon electrode and the size effect on their electrocatalytic activity toward oxygen reduction reaction (ORR) is investigated with electrochemical techniques in alkaline electrolyte. The cyclic voltammetric (CV) studies show that the onset potential of ORR on 0.7 nm silver nanoclusters is 150 mV more positive than that from 3.3 nm silver nanoparticles. And compared to the larger nanoparticles, five times higher current density of ORR at −0.80 V is obtained from the 0.7 nm silver nanoclusters. These CV results indicate that the smaller Ag nanoclusters exhibit higher catalytic performance for ORR. Rotating disk voltammetric studies show ORR on both DMSA monolayer-protected silver clusters is dominated first by a two-electron transfer pathway to produce H_2O_2 and then peroxide is reduced by 2 more electrons to produce water.

1. Introduction

Coin metals such as copper, silver and gold are usually considered to be very catalytically inert for most reactions. However, gold on nanocluster scale exhibits much higher catalytic activity than larger nanoparticles and bulk metal in many important reactions, such as low temperature CO oxidation and NO reduction [1–3], selective hydrosilylation [4], hydrogenation of acrolein [5]. The poor activity of coin metals (Au, Ag, Cu) is usually attributed to their filled d bands resulting in the higher activation barriers than those created for other transition metals with only partially filled d bands. For small nanoclusters, the fraction of low-coordinated atoms at surface remarkably increased. Due to the narrow gap between the d-band and the Fermi level of low-coordinated metal atoms, oxygen molecules could be adsorbed on the cluster surface more easily than the close-packed counterparts, which is the crucial step for organic molecules oxidation or oxygen reduction reactions. It is well-known that the fraction of surface atoms of metal nanoparticles is strongly dependent on the particle dimension. Therefore, several studies have been carried out to evaluate the effect of particle size on their catalytic activity. Recently, it was found that the Au nanoclusters exhibited size-dependent electrocatalytic activity for oxygen reduction [6,7].

Due to the high surface area and promoted catalytic activity of nanoparticles, the electrocatalysis of silver materials on nanometer scale has also attracted much attention in recent years. Based on the previous studies of ORR or hydrogen peroxide reduction with Ag materials [8,9], the average number of the electron transfers (n) is between 2 and 4, that is, the final products involve HO_2^- or OH. Yet, so far, the studies of the influence of the silver particle size on the electrocatalytic activity have been mostly confined to particles that are larger than 20 nm in diameter. The properties of small nanoclusters, especially below 10 nm, could be dramatically different from larger ones due to the quantum size effects. ORR electrocatalyzed by Ag nanoclusters with size smaller than 10 nm, however, is still scarce due to the difficulty in the synthesis of small Ag clusters. Recently, silver nanoclusters with controlled core size have been successfully synthesized by different methods, which makes it possible to study the electrocatalytic activity of Ag nanoclusters toward ORR. Here, we synthesized 0.7 and 3.3 nm silver nanoclusters by using different synthesis routes. The size effect of the Ag nanoclusters on their electrocatalytic activity for ORR was studied with electrochemical techniques.

2. Experimental

2.1. Chemicals

Silver nitrate was purchased from Beijing Chemical Reagent. Tetra-*n*-octylammonium bromide (TOABr, 98%) was obtained from

* Corresponding author. Tel.: +86 431 85262061; fax: +86 431 85262697.
E-mail address: weichen@ciac.jl.cn (W. Chen).

0378-7753/$ – see front matter © 2011 Elsevier B.V. All rights reserved.
doi:10.1016/j.jpowsour.2011.09.033

Alfa Aesar. Sodium borohydride, meso-2, 3-dimercapto-succinic acid (DMSA, approximately 98%), and potassium hydroxide were purchased from ACROS. All chemicals were used as received without any further purification. Water was supplied by a Water Purifier Nanopure water system (18.3 MΩ cm).

2.2. Synthesis of Ag nanoclusters

The thiol-protected Ag nanoclusters were synthesized according to the modified procedure reported previously by Jin and co-workers [10]. Precursor of [TOA][$AgBr_2$] was firstly synthesized as described before [11]. Briefly, DMSA (0.8 mmol, 146 mg) was added to the cold [TOA][$AgBr_2$] solution under stirring. $NaBH_4$ (10 mg, powders) was then dropwise added to the solution. The color of the reaction mixture slowly turned to deep brown, indicating the formation of thiolate-protected Ag clusters. The Ag nanoclusters were obtained by centrifugation and purification and then dissolved in water. The synthesized Ag nanoclusters coated with a monolayer of meso-2, 3-dimercapto-succinic acid (DMSA) are 0. 7 nm in diameter and denoted as Ag-NCs.

Larger silver nanoparticles were also synthesized with chemical reduction method. In a typical synthesis, $AgNO_3$ (0.2 mmol) was dissolved in 10 mL ethanol and then cooled to ~0 °C in an ice bath. Under the magnetic stirring with low speed ca. ~60 rpm, DMSA (0.4 mmol, 2 equiv.) was added to the above solution. After the complete formation of Ag_x $(DMSA)_y$ aggregates, $NaBH_4$ (20 mg) was slowly added to the solution. The resultant black precipitates were collected, washed thoroughly with ethanol, and finally dissolved in water for further use. The synthesized Ag nanoparticles are 3.3 nm in diameter and denoted as Ag-NPs. The size and the morphology of the Ag nanoparticles were examined by using Hitachi H-600 transmission electron microscopy (TEM) operated at 100 kV. UV–vis spectra of Ag-NCs and Ag-NPs were recorded on a VARIAN CARY 500 spectrometer using a 1 cm quartz cuvette with a resolution of 2 nm.

2.3. Electrochemistry

10 μL of the Ag-NPs or Ag-NCs in water (1 mg mL^{-1}) was then dropcast onto a clean GC electrode surface (3 mm diameter) by a microliter syringe and was dried by a gentle nitrogen flow for ca. 2 min. The resulting clean electrodes are denoted as Ag-NPs/GC and Ag-NCs/GC, respectively.

Voltammetric measurements were carried out with a CHI 750D electrochemical workstation. The Ag-NPs/GC and Ag-NCs/GC electrodes prepared above were used as the working electrodes. A Ag/AgCl (in 3 M NaCl, aq, +0.22 V vs NHE and ~+1.0 V vs RHE for pH = 13) and a Pt coil were used as the reference and counter electrodes, respectively. All electrode potentials in the present study were referred to this Ag/AgCl reference. 0.1 M KOH was used as electrolyte in all the electrochemical measurements. The rotating disk voltammograms on all electrodes were measured at the potential scan rate of 20 mV s^{-1}. Oxygen reduction was examined by first bubbling the electrolyte solution with ultrahigh purity oxygen for at least 15 min and then blanketing the solution with an oxygen atmosphere during the entire experimental procedure. All electrochemical experiments were carried out at room temperature.

3. Results and discussion

3.1. Synthesis of Ag nanoclusters with different core size

It is well known that metal, especially gold and silver nanoparticles exhibit characteristic surface plasmon absorption bands, with the band position and intensity dependent on the particle dimensions [12]. The previous investigations showed that large silver nanoparticles often exhibit an absorption band around 420 nm [13], whereas the small silver nanoclusters below 2 nm demonstrate different absorption profiles [14–16]. Thus, the size of silver nanoparticles can be evaluated qualitatively by the UV–vis measurements. Fig. 1(a) shows the UV–vis absorption spectra of the two synthesized silver nanoclusters. It can be seen that there is a broad absorption peak at 427 nm in the UV–vis spectrum (black curve) of the Ag-NPs, which is the characteristic of Ag nanoparticles. However, for the Ag-NCs, the absorption peak shifts to 503 nm (red curve), which is highly consistent with the UV–vis absorption feature of Ag_7 nanoclusters (ca. 0.7 nm) reported previously [10,17]. Fig. 1(b) shows the representative TEM micrograph of the silver nanoparticles (Ag-NPs). From the TEM measurement, it can be seen that the as-synthesized silver nanoparticles are all very well dispersed without any apparent aggregation. The average core diameter of the Ag-NPs is determined to be 3.3 nm from the TEM image.

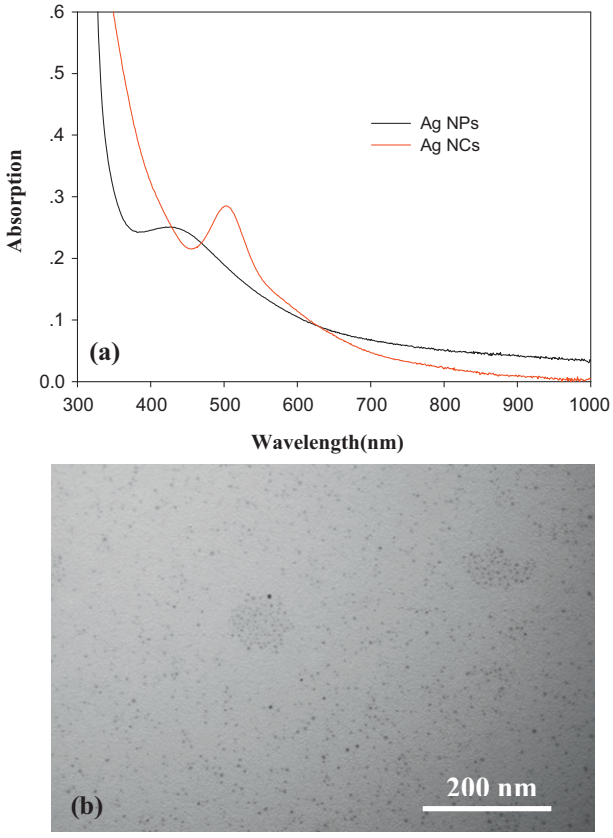

Fig. 1. (a) UV–vis absorption spectra of the silver nanoparticles (Ag-NPs, black curve) and silver nanoclusters (Ag-NCs, red curve). (b) TEM micrograph of the as-synthesized silver nanoparticles (Ag-NPs). (For interpretation of the references to color in this figure legend, the reader is referred to the web version of the article.)

3.2. Electrochemical cyclic voltammetry

The electrocatalytic activity of the silver nanoclusters toward ORR was then examined by CV. Fig. 2(a) and (b) shows the typical cyclic voltammograms (CVs) of Ag-NPs/GC and Ag-NCs/GC electrodes in 0.1 M KOH solution saturated with nitrogen or oxygen at potential scan rate of 0.1 V s^{-1}. On both electrodes, compared to the CVs in nitrogen saturated electrolyte, obvious reduction current can be observed when the KOH solution was saturated with oxygen, suggesting the high electrocatalytic activity of the silver nanoclusters toward oxygen reduction. It should be noted that in the CV and RDE measurements, the current of ORR on both electrodes have

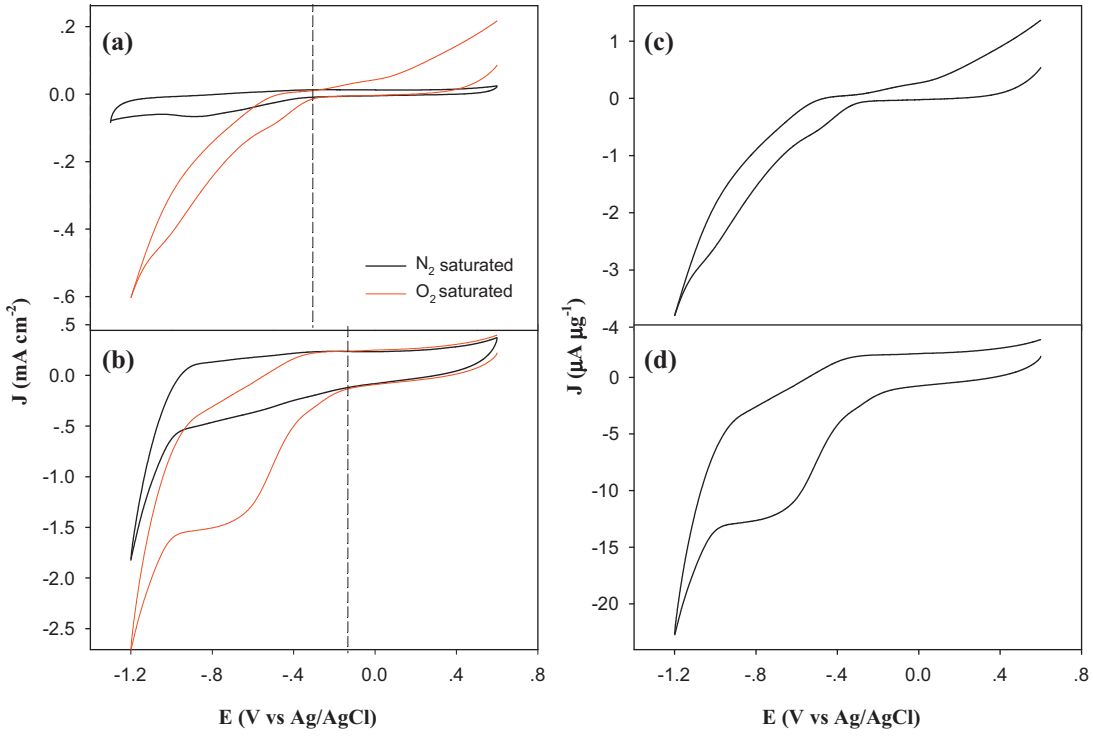

Fig. 2. Cyclic voltammograms of the Ag-NPs/GC (a) and Ag-NCs/GC (b) electrodes in 0.1 M KOH solution saturated with nitrogen (black curves) and oxygen (red curves), with the current normalized by the electrochemically active surface areas. Panels (c) and (d) depict the cyclic voltammograms of oxygen reduction at Ag-NPs and Ag-NCs, respectively, with the current normalized by the mass loading of the catalysts. Potential scan rate 0.1 V s^{-1}. (For interpretation of the references to color in this figure legend, the reader is referred to the web version of the article.)

been normalized to the real active surface areas (electrochemically active surface areas, ECASA) based on the charge density of 420 μC cm^{-2} for the reduction of the silver oxide. The electrocatalytic activities of the silver nanoclusters can be evaluated and compared with the onset potentials and current densities of ORR. It can be seen by comparing Fig. 2(a) and (b) that the two important parameters are much different at Ag-NPs/GC and Ag-NCs/GC electrodes. As for onset potential, −0.28 and −0.13 V were obtained at Ag-NPs/GC and Ag-NCs/GC electrodes, respectively. That means the onset potential of ORR on 0.7 nm silver nanoclusters is 150 mV more positive than that from 3.3 nm silver nanoparticles. At Ag-NPs/GC electrode, the oxygen reduction current density at −0.80 V was measured to be approximately −0.25 mA cm^{-2}. However, the peak current density of ORR at −0.80 V increases to −1.50 mA cm^{-2} at Ag-NCs/GC electrode, five times higher than that obtained on Ag-NPs/GC electrode. Fig. 2(c) and (d) shows the mass activities (current normalized by the mass loading of the catalysts) of the Ag-NPs and Ag-NCs toward ORR, respectively. From Fig. 2(c) and (d), it can also be seen that the smaller Ag-NCs exhibit higher mass activity than that obtained from the larger Ag-NPs. For instance, at −0.76 V, the current density of −12.48 μA $μg^{-1}$ was obtained at Ag-NCs, which is about 9.2 times higher than that of the Ag-NPs (−1.36 μA $μg^{-1}$). The voltammetric studies showed clearly that the electrocatalytic activity of smaller Ag nanoclusters toward ORR is higher than the larger one, which is in accordance with our previous finding with gold nanoclusters [6].

To obtain the kinetic parameters of ORR on silver nanoclusters, the reaction kinetic of oxygen reduction at the silver nanoclusters were also studied with rotating disk voltammetry (RDV). Fig. 3 shows a series of RDVs of ORR recorded at Ag-NPs/GC (Fig. 3a) and Ag-NCs/GC (Fig. 3b) at different rotation rates (225, 400, 625, 900, 1225, 1600, 2025, 2500, 3025 and 3600 rpm). It can be seen that on both electrodes, the limiting current density increases with rotation rate increasing. Again, the similar voltammetric profiles displayed in Fig. 3(a) and (b) suggest the apparent activity of the synthesized silver nanoclusters toward ORR.

The kinetic parameters of ORR on the silver nanoclusters can be analyzed with the Koutecky–Levich equations:

$$\frac{1}{J} = \frac{1}{J_K} + \frac{1}{J_L} = \frac{1}{J_K} + \frac{1}{B\omega^{1/2}} \quad (1)$$

$$B = 0.62nFC_O D_O^{1/3} \nu^{-1/6} \quad (2)$$

$$J_K = nFkC_O \quad (3)$$

According to Eqs. (1) and (2), the number of electrons transferred can be obtained from the slope of the Koutecky–Levich plots. Based on the Koutecky–Levich equations, the corresponding Koutecky–Levich plots on the two electrodes are shown in Fig. 3(a) and (b) insets. It can be seen that the slopes remain approximately constant over the potentials range from −0.70 to −0.90 V, indicating consistent numbers of electron transfer for ORR at different electrode potentials. By using the reported values of $C_O = 1.2 \times 10^{-3}$ mol L^{-1}, $D_O = 1.9 \times 10^{-5}$ cm^2 s^{-1}, and $\nu = 0.01$ cm^2 s^{-1} [18], and from the slopes of Koutecky–Levich plots, the numbers of electrons transferred were determined to be 2.8 and 2.3, respectively, for ORR on Ag-NPs/GC and Ag-NCs/GC electrodes. Additionally, on the basis of Eq. (3), the reaction rate constants at −0.70 V can be assessed to be 1.22×10^{-2} and 3.24×10^{-3} cm s^{-1} on Ag-NPs/GC and Ag-NCs/GC electrodes, respectively. The RDE results indicate that the oxygen reduction on the synthesized silver clusters is mainly dominated by a two-electron transfer pathway to produce H_2O_2 and then peroxide is reduced by 2 more electrons to produce water. It should be noted that, in order to prevent the agglomeration of the silver nanoclusters, the protecting ligands were not removed during the electrochemical measurements. The low interfacial charge transfer obtained in RDVs may be ascribed to the passivated surfaces of the silver nanoclusters.

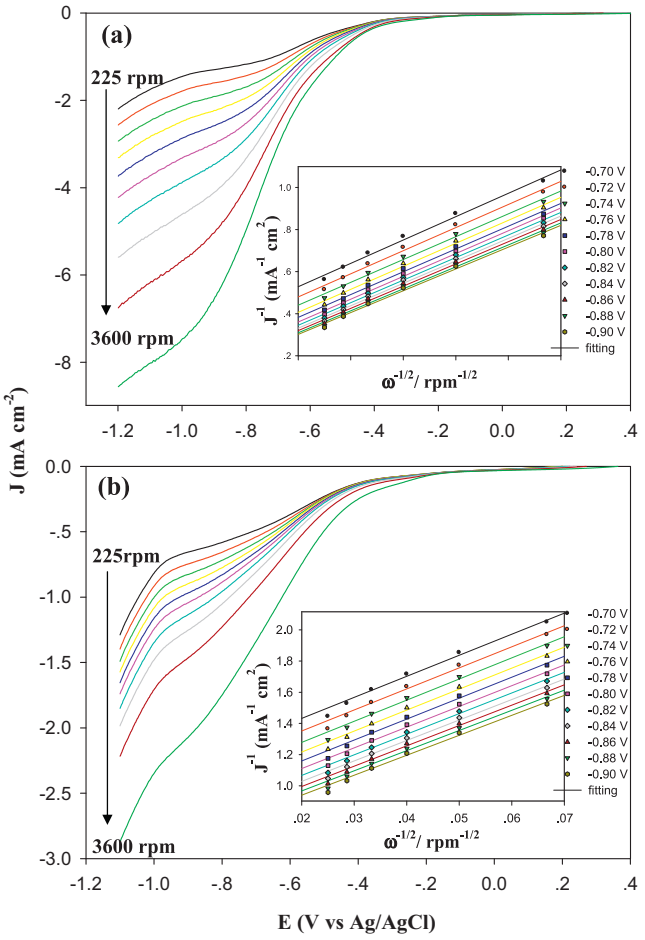

Fig. 3. Rotating-disk voltammograms obtained on the Ag-NPs/GC (a) and Ag-NCs/GC (b) electrodes in 0.1 M KOH solution saturated with oxygen at different rotation rates (shown as figure legends). Insets show the corresponding Koutecky–Levich plots (J^{-1} vs $\omega^{-1/2}$) at different potentials. Symbols are experimental data obtained from the corresponding Rotating-disk voltammograms and lines are the linear regressions.

4. Conclusion

Silver nanoclusters with different core sizes were synthesized successfully with meso-2, 3-dimercapto-succinic acid as protecting ligands. The size effect of the synthesized silver nanoclusters on the electrocatalytic activity for ORR was investigated with CV and RDV in alkaline electrolyte. The CV studies indicate that the 0.7 nm Ag_7 clusters exhibit better electrocatalytic activity than that of 3.3 nm Ag nanoparticles by comparing the onset potential and current densities of ORR. Two-electron reduction process of adsorbed oxygen was derived from the kinetic results of RDV, and the two-electron transfer pathway shown in this study may be ascribed to the capping ligand-passivated surfaces of the silver nanoclusters.

Acknowledgements

This work was supported by the National Natural Science Foundation of China (No. 21043013) and the startup funds for scientific research, Changchun Institute of Applied Chemistry, Chinese Academy of Sciences.

References

[1] G.C. Bond, D.T. Thompson, Catalysis Reviews-Science and Engineering 41 (1999) 319.
[2] M. Haruta, Catalysis Today 36 (1997) 153.
[3] C.J. Kiely, A.A. Herzing, A.F. Carley, P. Landon, G.J. Hutchings, Science 321 (2008) 1331.
[4] A. Corma, C. Gonzalez-Arellano, M. Iglesias, F. Sanchez, Angewandte Chemie-International Edition 46 (2007) 7820.
[5] P. Claus, A. Bruckner, C. Mohr, H. Hofmeister, Journal of the American Chemical Society 122 (2000) 11430.
[6] W. Chen, S.W. Chen, Angewandte Chemie-International Edition 48 (2009) 4386.
[7] W. Tang, H.F. Lin, A. Kleiman-Shwarsctein, G.D. Stucky, E.W. McFarland, Journal of Physical Chemistry C 112 (2008) 10515.
[8] A. Kongkanand, S. Kuwabata, Electrochemistry Communications 5 (2003) 133.
[9] R.G. Compton, F.W. Campbell, S.R. Belding, R. Baron, L. Xiao, Journal of Physical Chemistry C 113 (2009) 9053.
[10] Z.K. Wu, E. Lanni, W.Q. Chen, M.E. Bier, D. Ly, R.C. Jin, Journal of the American Chemical Society 131 (2009) 16672.
[11] P.J.G. Goulet, R.B. Lennox, Journal of the American Chemical Society 132 (2010) 9582.
[12] K.P. Charle, W. Schulze, B. Winter, Zeitschrift Fur Physik D-Atoms Molecules and Clusters 12 (1989) 471.
[13] M.C. Tong, W. Chen, J. Sun, D. Ghosh, S.W. Chen, Journal of Physical Chemistry B 110 (2006) 19238.
[14] J.G. Zhang, S.Q. Xu, E. Kumacheva, Advanced Materials 17 (2005) 2336.
[15] A. Banerjee, B. Adhikari, Chemistry of Materials 22 (2010) 4364.
[16] T.P. Bigioni, S. Kumar, M.D. Bolan, Journal of the American Chemical Society 132 (2010) 13141.
[17] O. Zaluzhna, L. Brightful, T.C. Allison, Y.Y. Tong, Chemical Physics Letters 509 (2011) 148.
[18] Y.Z. Lu, Y.C. Wang, W. Chen, Journal of Power Sources 196 (2011) 3033.